

**GENERALIZED FORCES AND DISSIPATION FUNCTIONS
IN THE CONTEXT OF AN INTERNAL VARIABLE APPROACH
APPLIED TO THE SOLUTION OF ELASTIC-PLASTIC PROBLEMS**

Alfonso Nappi¹, Daniele Zaccaria²

¹Professor, ²Associate Professor

Department of Engineering and Architecture

University of Trieste, P.le Europa 1, 34127 Trieste, Italy

nappi@units.it

Abstract

A non-traditional approach to the numerical analysis of elastic-plastic systems is discussed by focusing on a formulation that makes use of *internal variables* and *dissipation functions*. These functions are used in order to enforce the constitutive law, so that they play the role of the *yield functions* in the framework of the classical *theory of plasticity*.

With reference to finite element discrete models, it is shown that the solution of an elastic-plastic problem corresponds to the minimum point of a convex function (when the material is stable in *Drucker's sense*) and that convergence is guaranteed when a convenient time integration method (usually known as *backward-difference* scheme) is applied. As a matter of fact, it can be proved that the value of that function progressively decreases (iteration by iteration) when a proper time integration strategy is implemented.

Elastic-plastic systems will be considered, which are subjected to uniaxial and multiaxial stress states (by assuming Mises' yield condition for two-dimensional and three-dimensional finite elements). In all cases, it will be easily noticed that the *dissipation functions* depend on convenient *generalized forces*, whose features are obvious in the presence of uniaxial stress states. Instead, when the structural system is subjected to multiaxial stress states, the actual meaning of the *generalized forces* must be properly understood in order to define convenient *dissipation functions* and/or *yield functions*: this is the main issue of the present paper and represents a topic which, to the authors' knowledge, has not been adequately investigated, yet.

Keywords: Backward-difference, Convergence, Convex analysis, Discrete models, Dissipation functions, Elastic-plastic materials, Finite element method, Internal variables, Iterative schemes.

1. Introduction

This work is essentially based on the numerical solution of elastic-plastic problems on the basis of a non-traditional approach that was originally developed by Martin [1]. It makes use of the so-called *internal variables* (*i.e.*, non-measurable variables), which, in this case, represent non-reversible plastic strains or displacements. Perhaps more importantly, this approach does not make use of the classical *yield functions*. Instead, the constitutive law is enforced by introducing adequate *dissipation functions*, which allow one to determine the correct values of the stresses by considering either the derivatives or the subdifferentials of these functions.

The key feature of the *internal variable approach* discussed here is that the solution of an incremental elastic-plastic problem coincides with the minimum point of a convex non-constrained objective function, say ω , when typical conditions are met:

- the equilibrium equations are written with reference to the initial, undeformed configuration
- the material is stable in *Drucker's sense* (*i.e.*, is characterized by a convex yield function and an associated flow rule, which implies incremental plastic strain rates that are normal to the yield surface)

As for the *incremental elastic-plastic problem*, it should be observed that we refer to the usual discrete, finite element models of elastic-plastic systems, which are subjected to given load

histories subdivided into a finite number of time-steps. Of course, the objective is to compute the solutions in terms of incremental displacements, strains, plastic strains and stresses when these quantities are known at the beginning of a certain time-step Δt (*i.e.*, at the end of the previous one). For this kind of problem, it can also be proved that an iterative procedure based on an implicit iterative method, usually known as *backward-difference* scheme, ensures that the value of the function ω steadily decreases (iteration by iteration) when we compute the solution concerned with a given time-step. Therefore, convergence is guaranteed.

It is worth noting that, in this context, the *backward-difference* scheme denotes a numerical technique, which eventually provides finite increments of the plastic strain vectors that are normal to the yield surface at the point that represents the current stress. In other words, whenever a non-zero incremental plastic strain vector $\Delta \epsilon^P$ occurs, the direction of $\Delta \epsilon^P$ must coincide with the direction of the gradient $\partial \phi / \partial \sigma$ of the yield function $\phi(\sigma) = 0$, if this gradient is computed for $\sigma = \sigma^*$, where $\sigma^* = \sigma^o + \mathbf{D}(\Delta \epsilon - \Delta \epsilon^P)$ is the stress vector at the end of the current time-step, σ^o the stress vector at the end of the previous time-step, \mathbf{D} the material elastic stiffness matrix and $\Delta \epsilon$ the vector whose entries denote the total incremental strains.

In the literature, further details can be found on the general features of the *internal variable* approach [2] and on the convergence properties of algorithms based on the *backward-difference* scheme in the presence of quasi-static [3] and dynamic [4] load conditions.

Here, we will discuss uniaxial and multiaxial stress states. While dealing with multiaxial stress states, we will confine our attention to linear kinematic or isotropic hardening and elastic-plastic systems for which Mises' yield condition is applicable. However, the extension to more general materials is possible.

The main topic of the paper, however, is the role played by *generalized forces*, which are related to the reversible (elastic) strains and must be taken into account in order to define the function ω mentioned above. Indeed, there is a close connection between these *generalized forces* and the *dissipation functions*, which are key elements of the function ω and are needed to compute the correct values of the plastic strain increments.

To the best of the authors' knowledge, the features of these *generalized forces* have been neglected so far, but they definitely deserve some attention. In fact, while everything is obvious and straightforward in the case of uniaxial stress states, there are some non-trivial issues that should be considered and properly understood, when the *internal variable* approach discussed here is applied in the context of numerical methods for structural analysis.

2. Internal variables and uniaxial stress states

This Section is concerned with the fundamentals of an *internal variable* approach to the description of the response of an elastic-plastic structure. We will start by considering the mechanical model of an elastic-perfectly plastic system subjected to a uniaxial stress state (*cf.* Fig. 1).

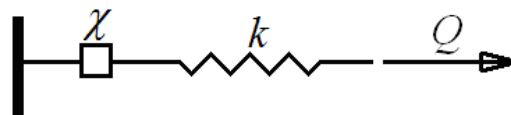


Figure 1. Mechanical model for elastic perfectly-plastic systems.

This mechanical model consists of a rigid perfectly-plastic slip device and a linear elastic spring. Let us start with the slip device, schematically denoted by a square in Fig. 1. As shown in Fig. 2, it behaves like a rigid element, when it is subjected to a load $\chi < \chi^+$ and $\chi > \chi^-$. Instead, when $\chi = \chi^+$ or $\chi = \chi^-$, unlimited plastic elongations λ are assumed to be possible. Therefore, for any $\lambda \neq 0$, the energy $D = \chi^- \lambda$ or $D = \chi^+ \lambda$ is dissipated (cf. Fig. 3).

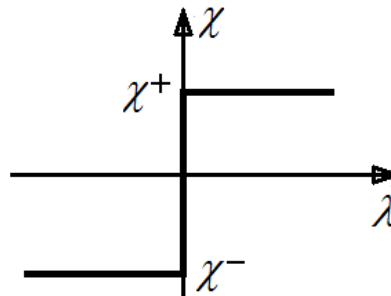


Figure 2. Typical χ - λ plot for a slip device.

The *dissipation function* has an interesting feature, which is quite evident in Fig. 3. Indeed, if we consider the subdifferential of D (i.e., the set of subgradients of D at $\lambda = 0$ or, in other words, the slopes of the straight lines that pass through the origin without intersecting the graph), we notice that χ must be an element of that subdifferential for $\lambda = 0$. Instead, for $\lambda \neq 0$, χ corresponds to the derivative of $D(\lambda)$. Thus, we can state that $\chi \in \partial D(\lambda)$ for $\lambda = 0$, while $\chi = dD/d\lambda$ for $\lambda \neq 0$.

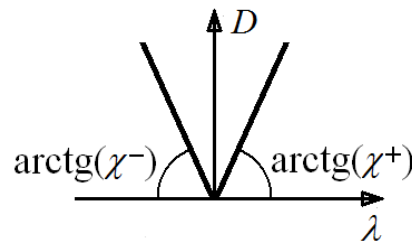


Figure 3. Dissipation function.

Let us now turn back to the mechanical model in Fig. 1. Since the slip device and the linear elastic spring, whose stiffness is k , are connected in series, that model represents an elastic perfectly-plastic system. In fact, its response must be linear elastic if $\chi^- < \chi < \chi^+$, while λ can attain any value if $\chi = \chi^+$ or $\chi = \chi^-$.

Instead, if $\chi = \chi^+$ and we unload the system, its response must be linear elastic, unless we increase the load again (up to $\chi = \chi^+$) or unless we continue to decrease the load until $\chi = \chi^-$. In any case, whatever we do, the equilibrium equation reads $Q = k(q - \lambda)$. Here, q denotes the displacement of the free end (i.e., the elongation of the mechanical model), while λ plays the role of an *internal variable* (i.e., a quantity that cannot be measured directly). As pointed out before, the response is typical of bars consisting of elastic perfectly-plastic materials. However, the constitutive law is imposed by introducing a relationship between the non-reversible plastic strains and a *dissipation*

function, instead of using inequality constraints (i.e., yield functions), as typical of classical descriptions of elastic plastic systems.

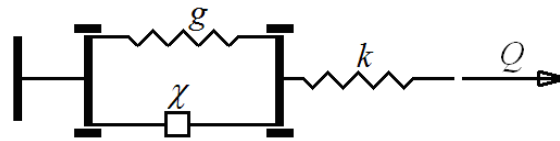


Figure 4. Mechanical model for systems characterized by linear kinematic hardening.

The above model can be developed in order to describe the behavior of an elastic plastic system subjected to kinematic hardening. An example is given in Fig. 4, where we have introduced a second elastic spring. If its response is linear elastic (i.e., if the stiffness g is constant) we eventually have a mechanical model characterized by linear hardening.

In fact, the elongation of the second spring must be equal to the elongation of the slip device, since the vertical rigid bars are forced to remain parallel (and the slip device cannot be subjected to any relative displacement unless $\chi = \chi^+$ or $\chi = \chi^-$).

In order to better understand the response of the model, we can consider the plot of Fig. 5. It is easily possible to check that the model of Fig. 4 gives this plot if we set $k=20$ kN/mm, $\chi^+=20$ kN and $g=6.66667$ kN/mm.

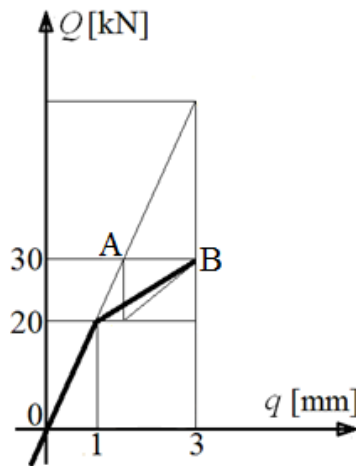


Figure 5. Typical Q - q plot for a system characterized by linear hardening.

As a matter of fact, for $Q \leq 20$ kN, we have $Q = \chi$, since the slip implies $\lambda = 0$ and the second spring cannot be subjected to any change of configuration. Meanwhile, the displacement q corresponds to the elongation of the first spring and we obtain $Q = kq$.

When $Q > \chi^+ = 20$ kN, the second spring must be subjected to the force $\varphi = Q - \chi^+$, since the slip cannot be loaded with a force greater than χ^+ . At this stage, we can also notice that $\varphi = g\lambda$, since the elongation of the slip device must be equal to the elongation of the second spring.

In addition, we have $\varphi = 6.66667 \times 1.5 = 10$ kN when λ is equal to 1.5 mm (which corresponds to the segment AB). This means that the displacement of the free end, q , must be equal to 3 mm. In fact,

the equation $Q=k(q-\lambda)$ and the relationship $\varphi=Q-\chi^+=g\lambda$ can only be satisfied for $q=3$ mm and $\lambda=1.5$ mm, since the force acting on the slip device cannot exceed 20 kN.

That said, we immediately see that a linear elastic path is followed, if the system is unloaded. Indeed, if we decrease the force Q after reaching point B, this fact necessarily implies $q<3$ mm, while λ and φ must remain constant (φ cannot diminish unless λ decreases, but, in turn, λ cannot decrease unless $\chi=\chi^-$).

More precisely, λ can only change if we reload the system (until $\chi=\chi^+$) or we continue to add negative increments to Q (until $\chi=\chi^-$). Thus, we shall always have a linear elastic response in a range given by $\chi^+-\chi^-$. Therefore, the mechanical model of Fig. 4 is actually concerned with an elastic plastic system characterized by *linear kinematic hardening*.

Let us now consider a structural system consisting of e elastic-hardening elements, such as the one in Fig. 4. When the small displacement theory is applied, we easily derive the equilibrium equation

$$\mathbf{F} = \mathbf{K} \mathbf{U} + \mathbf{L} \boldsymbol{\lambda} \quad (1)$$

Indeed, if we assume n degrees of freedom and e structural elements, the vectors \mathbf{F} , \mathbf{U} , $\boldsymbol{\lambda}$ collect n given loads, n displacement components and e plastic, non reversible displacements. Therefore, by introducing the vectors \mathbf{q} and \mathbf{Q} , which collect the elongations q_i of the e structural elements ($i=1, \dots, e$) and their axial forces $Q_i=k_i(q_i-\lambda_i)$, the equilibrium and compatibility equations read

$$\mathbf{q} = \mathbf{C} \mathbf{U} \quad , \quad \mathbf{F} = \mathbf{C}^T \mathbf{Q} \quad (2a,b)$$

Hence, by defining a diagonal matrix $\mathbf{S}=\text{diag}[k_i]$ such that $\mathbf{Q}=\mathbf{S}(\mathbf{q}-\boldsymbol{\lambda})$, we immediately obtain $\mathbf{K}=\mathbf{C}^T \mathbf{S} \mathbf{C}$ and $\mathbf{L}=-\mathbf{C}^T \mathbf{S}$.

In view of some further issues that will be discussed later, we should also observe that the product $\mathbf{L}^T \mathbf{U}=-\mathbf{S} \mathbf{C} \mathbf{U}$ gives a vector, which represents the axial forces (with the sign changed) that would be applied to the structural system, if the response to the displacement vector \mathbf{U} were linear elastic. Next, by collecting the forces acting on the e slips into a vector $\boldsymbol{\chi}$, we can set

$$\boldsymbol{\chi} = \mathbf{Q} - \boldsymbol{\varphi} = \mathbf{S}(\mathbf{q} - \boldsymbol{\lambda}) - \mathbf{G} \boldsymbol{\lambda} \quad (3)$$

where $\boldsymbol{\varphi}$ represents the e forces acting on the springs, which are in parallel with the slips, as typical of the mechanical model in Fig. 4, while $\mathbf{G}=\text{diag}[g_i]$ collects the stiffness parameters that characterize these springs.

From eqn. (3) we derive the relationship

$$-\boldsymbol{\chi} = \mathbf{L}^T \mathbf{U} + \mathbf{S} \boldsymbol{\lambda} + \mathbf{G} \boldsymbol{\lambda} \quad (4)$$

In view of the governing equations (1) and (4), we can state that the solution of the elastic-plastic problem for a given load vector \mathbf{F} corresponds to the minimum point of the function

$$\omega(\mathbf{U}, \boldsymbol{\lambda}) = \frac{1}{2} \mathbf{U}^T \mathbf{K} \mathbf{U} + \frac{1}{2} \boldsymbol{\lambda}^T \mathbf{S} \boldsymbol{\lambda} + \frac{1}{2} \boldsymbol{\lambda}^T \mathbf{G} \boldsymbol{\lambda} + \mathbf{U}^T \mathbf{L} \boldsymbol{\lambda} + D(\boldsymbol{\lambda}) - \mathbf{F}^T \mathbf{U} \quad (5)$$

where $D(\boldsymbol{\lambda})$ denotes the dissipation function of the entire structure.

As a matter of fact, eqn. (1) is obtained by deriving $\omega(\mathbf{U}, \boldsymbol{\lambda})$ with respect to \mathbf{U} and setting this derivative equal to zero. Similarly, we can take the derivative of $\omega(\mathbf{U}, \boldsymbol{\lambda})$ with respect to $\boldsymbol{\lambda}$ (when possible) and set this derivative equal to zero in order to recover eqn. (4). Of course, for each $\lambda_i=0$, we shall consider a convenient element of the subdifferential of $D(\boldsymbol{\lambda})$, instead of the derivative of $D(\boldsymbol{\lambda})$ with respect to λ_i . Namely, we can state that $\chi_i=\partial D/\partial \lambda_i$ if $\lambda_i \neq 0$, while $\chi_i \in \partial D(\boldsymbol{\lambda})$ if $\lambda_i=0$.

Note that $\omega(\mathbf{U}, \boldsymbol{\lambda})$ is positive definite thanks the contribution given by $\frac{1}{2} \boldsymbol{\lambda}^T \mathbf{G} \boldsymbol{\lambda}$, which is due to the linear hardening behavior of the structural elements.

In general, an elastic plastic problem is solved by subdividing the load history into a finite number of time-steps. Consequently, eqns. (1) and (4) can be rewritten in the form

$$\mathbf{F}_0 + \Delta \mathbf{F} = \mathbf{K} \{\mathbf{U}_0 + \Delta \mathbf{U}\} + \mathbf{L} \{\boldsymbol{\lambda}_0 + \Delta \boldsymbol{\lambda}\} \quad , \quad -\boldsymbol{\chi} = \mathbf{L}^T \{\mathbf{U}_0 + \Delta \mathbf{U}\} + \mathbf{S} \{\boldsymbol{\lambda}_0 + \Delta \boldsymbol{\lambda}\} + \mathbf{G} \{\boldsymbol{\lambda}_0 + \Delta \boldsymbol{\lambda}\} \quad (6a,b)$$

having set $\mathbf{U}_0 + \Delta \mathbf{U} = \mathbf{U}$, $\mathbf{F}_0 + \Delta \mathbf{F} = \mathbf{F}$, $\boldsymbol{\lambda}_0 + \Delta \boldsymbol{\lambda} = \boldsymbol{\lambda}$, where $\Delta \mathbf{U}$, $\Delta \mathbf{F}$, $\Delta \boldsymbol{\lambda}$ refer to the increments concerned with a certain time-step, while \mathbf{U}_0 , \mathbf{F}_0 , $\boldsymbol{\lambda}_0$ denote the values attained by the same quantities at the end of the previous time-step.

In consequence, the convex function whose minimum point coincides with the solution of the incremental elastic plastic problem becomes

$$\begin{aligned} \omega^*(\Delta \mathbf{U}, \Delta \boldsymbol{\lambda}) = & \frac{1}{2} \Delta \mathbf{U}^T \mathbf{K} \Delta \mathbf{U} + \frac{1}{2} \Delta \boldsymbol{\lambda}^T \mathbf{S} \Delta \boldsymbol{\lambda} + \frac{1}{2} \Delta \boldsymbol{\lambda}^T \mathbf{G} \Delta \boldsymbol{\lambda} + \Delta \mathbf{U}^T \mathbf{L} \Delta \boldsymbol{\lambda} - \Delta \mathbf{F}^T \Delta \mathbf{U} + \\ & + D(\Delta \boldsymbol{\lambda}) + \Delta \mathbf{U}^T \{\mathbf{K} \mathbf{U}_0 + \mathbf{L} \boldsymbol{\lambda}_0 - \mathbf{F}_0\} + \Delta \boldsymbol{\lambda}^T \{\mathbf{L}^T \mathbf{U}_0 + \mathbf{S} \boldsymbol{\lambda}_0 + \mathbf{G} \boldsymbol{\lambda}_0\} \end{aligned} \quad (7)$$

3. Internal variables and multiaxial stress states

Relationships, which are formally identical to eqns. (1, 4, 6, 7) can be derived by considering multiaxial stress states, as shown in this Section, with special attention given to Mises' yield condition and to materials, which are either elastic-perfectly plastic or subjected to kinematic or isotropic hardening.

Since the main objective of the paper is the discussion of issues related to numerical solutions, we can start by considering the equation of virtual works applied to a structural system discretized by e finite elements

$$\sum_i \int \boldsymbol{\sigma}^T \delta \boldsymbol{\varepsilon} dV = \sum_i \int \mathbf{b}^T \delta \mathbf{u} dV + \sum_i \int \mathbf{f}^T \delta \mathbf{u} dS \quad (8)$$

where the vectors \mathbf{u} , $\boldsymbol{\varepsilon}$, $\boldsymbol{\sigma}$, \mathbf{b} and \mathbf{f} refer to displacements, strains, stress, body forces and surface forces respectively, while the integrals are to be computed by considering either the volume V_i or the surface S_i of each element (of course, with $\mathbf{f}=\mathbf{0}$ when an element face does not belong to the surface of the continuum or when it is not loaded).

By introducing the element stiffness matrix \mathbf{D}_i , together with the matrices $\boldsymbol{\Phi}_i$ and \mathbf{B}_i (which contain shape functions and convenient derivatives of these functions, respectively), we can set

$$\delta \mathbf{u} = \boldsymbol{\Phi}_i \delta \mathbf{u}_i \quad , \quad \delta \boldsymbol{\varepsilon} = \mathbf{B}_i \delta \mathbf{u}_i \quad , \quad \boldsymbol{\sigma} = \mathbf{D}_i \{\boldsymbol{\varepsilon} - \boldsymbol{\varepsilon}^p\} = \mathbf{D}_i \{\mathbf{B}_i \mathbf{u}_i - \boldsymbol{\Psi}_i \boldsymbol{\lambda}_i\} \quad (9a,b,c)$$

where \mathbf{u}_i denotes a vector of nodal displacements, while $\boldsymbol{\varepsilon}^p$ refers to plastic strains, which can either be constant within the i -th element or depend on their values at selected *strain points* (e.g., *Gauss points*) inside the element. In general, we can set $\boldsymbol{\varepsilon}^p = \boldsymbol{\Psi}_i \boldsymbol{\lambda}_i$, if $\boldsymbol{\Psi}_i$ is a matrix of convenient shape functions and $\boldsymbol{\lambda}_i$ is a vector, which collects the values attained by the plastic strains at the *strain points* of the i -th element. Of course, $\boldsymbol{\Psi}_i = \mathbf{I}$ (identity matrix), when $\boldsymbol{\varepsilon}^p$ is assumed to be constant (and the center of gravity of the element can be interpreted as a unique *strain point*).

If the contributions of the vectors $\boldsymbol{\lambda}_i$ were neglected, from eqn. (8) it would be possible to derive the classical relationship $\mathbf{K} \mathbf{U} = \mathbf{F}$ through the usual assembly process. As a matter of fact, we would obtain the equation $\delta \mathbf{U}^T \mathbf{K} \mathbf{U} = \delta \mathbf{U}^T \mathbf{F}$, to be satisfied for any set of virtual displacements (with \mathbf{U}

denoting the vector of all nodal displacements referred to a global coordinate system, while the vectors \mathbf{u}_i are often referred to local coordinate systems).

Instead, in the case of elastic-plastic structures, it is necessary to consider the integrals

$$\sum_i \int \{-\mathbf{D}_i \boldsymbol{\Psi}_i \boldsymbol{\lambda}_i\}^T \delta \boldsymbol{\varepsilon} dV = \sum_i \int \{\delta \mathbf{u}_i\}^T [-\mathbf{B}_i^T \mathbf{D}_i \boldsymbol{\Psi}_i] \boldsymbol{\lambda}_i dV = \sum_i \{\delta \mathbf{u}_i\}^T \mathbf{L}_i \boldsymbol{\lambda}_i \quad (10)$$

Thus, we eventually obtain the relationship $\mathbf{F}=\mathbf{K}\mathbf{U}+\mathbf{L}\boldsymbol{\lambda}$, which is formally identical to eqn. (1). Of course, the vector $\boldsymbol{\lambda}$ in this equation consists of the e subvectors $\boldsymbol{\lambda}_i$ and the matrix \mathbf{L} (obtained by assembling the submatrices \mathbf{L}_i) is part of the product $(\delta \mathbf{U}^T \mathbf{L} \boldsymbol{\lambda})$, which gives a further contribution (due to the inelastic strains) to the internal virtual work.

It can be easily noticed that the product $\{\mathbf{D}_i \mathbf{B}_i \mathbf{u}_i\}$ represents the stresses in the i -th element that would be given by the displacements \mathbf{u}_i if the structural response were fully elastic. In consequence, the products $\{\mathbf{L}_i^T \mathbf{u}_i\}$ and $\{\mathbf{L}^T \mathbf{U}\}$ represent *generalized forces* (with the sign changed) that would occur at the element level or at the structural level if the response to \mathbf{u}_i or \mathbf{U} were linear elastic.

As discussed later with some further details, these forces can be interpreted as fictitious concentrated loads that turn out to be equivalent to the stresses acting in a certain zone around a *strain point*. Of course, if an element is characterized by a single *strain point*, the relevant *generalized forces* must be equivalent to the stresses acting in the entire element.

It is also worth noting that the expression *generalized forces*, in general, is referred to quantities that give a contribution to some work or energy when we take the scalar product with a properly chosen vector (which, in this specific case, is the vector of plastic strains).

Now, we should observe that the *generalized forces* $\boldsymbol{\chi}_i = \{-\mathbf{L}_i^T \mathbf{u}_i\}$ can also represent the actions on fictitious slip devices ideally located at the *strain points* of each element until the structural response is linear elastic.

When plastic strains occur, these *generalized forces* become $\boldsymbol{\chi}_i = \{-\mathbf{L}_i^T \mathbf{u}_i - \mathbf{S}_i \boldsymbol{\lambda}_i\}$, if the material is elastic-perfectly plastic and \mathbf{S}_i represents a convenient stiffness matrix that plays the role of the stiffness parameter k concerned with the mechanical model subjected to uniaxial stress states. For the same reason, when linear hardening occurs, the *generalized forces* acting on the slip device become $\boldsymbol{\chi}_i = \{-\mathbf{L}_i^T \mathbf{u}_i - \mathbf{S}_i \boldsymbol{\lambda}_i - \mathbf{G}_i \boldsymbol{\lambda}_i\}$, where \mathbf{G}_i denotes a hardening matrix.

Therefore, the usual assembly process will lead to the relationship $-\boldsymbol{\chi} = \mathbf{L}^T \mathbf{U} + \mathbf{S} \boldsymbol{\lambda} + \mathbf{G} \boldsymbol{\lambda}$, formally identical to eqn. (4). In consequence, by introducing a proper dissipation function $D(\boldsymbol{\lambda})$, we can consider convex objective functions $\omega(\mathbf{U}, \boldsymbol{\lambda})$ or $\omega^*(\Delta \mathbf{U}, \Delta \boldsymbol{\lambda})$, fully analogous to the ones defined in eqns. (5) and (7), whose minimum points coincide with the solutions of given elastic plastic problems.

In addition, as already proved for structures subjected to quasi-static load conditions [3] and for dynamic systems [4], it is possible to guarantee the convergence of an iterative scheme based on the *backward-difference* concept, which essentially consists in determining (at each time-step) incremental plastic strains $\Delta \boldsymbol{\lambda}_i$ normal to the yield surfaces at the points that correspond to the final stresses $\{\boldsymbol{\sigma}^0 + \mathbf{D}_i \{\mathbf{B}_i \Delta \mathbf{u}_i - \boldsymbol{\Psi}_i \Delta \boldsymbol{\lambda}_i\}\}$ at the end of the current time-step (if $\boldsymbol{\sigma}^0$ denotes the stress vector at the end of the previous step at a certain *strain point*, while the matrices \mathbf{B}_i and $\boldsymbol{\Psi}_i$ are computed at the same *strain point*).

Of course, most of the times it is not straightforward to define a *dissipation function* and satisfy the conditions required by the *backward-difference* strategy. However, everything is quite easy when Mises' yield criterion is applicable and the material is either elastic-perfectly plastic or characterized by linear isotropic or kinematic hardening, as shown below.

We can start by focusing on an elastic-perfectly plastic material and observe that the relevant yield surface in the space of the deviatoric stresses is spherical, because it can be defined by considering the limit value, say w_L , of the distortion energy $\frac{1}{2}s_{ij}e_{ij}$, where s_{ij} and e_{ij} denote deviatoric stresses and strains, respectively. Since $s_{ij}=2Ge_{ij}$ for linear elastic isotropic materials, we obtain

$$\varphi(s_{hk}) = s_{ij} s_{ij} - 4 G w_L = s_{ij} s_{ij} - r^2 = 0 \tag{11}$$

Therefore, by expressing the *dissipation function* in terms of incremental plastic strains Δe_{ij}^p ($=\Delta e_{ij}^p$, since plastic strains are deviatoric in the case of Mises' yield condition), we can set $D(\Delta e_{ij}^p)=\hat{s}_{ij} \Delta e_{ij}^p$, if the deviatoric stresses \hat{s}_{ij} represent the coordinates of the point at which the incremental plastic strain occurs (*cf.* Fig. 6).

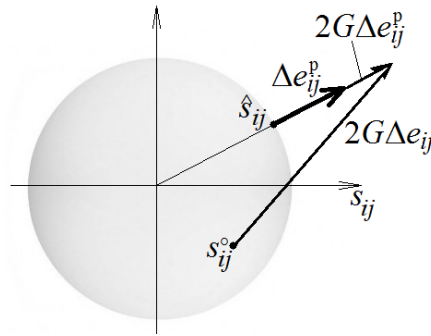


Figure 6. Mises' yield condition: elastic domain in the space of the deviatoric stresses.

Fig. 6 also gives a schematic view of what happens at a *strain point* when the *backward-difference* integration scheme is applied. At the beginning of each time-step, it is possible to compute the increment of the displacement vector $\Delta \mathbf{U}$ by assuming $\Delta \boldsymbol{\lambda}=\mathbf{0}$. Then, at each *strain point* we can compute the stresses $(\boldsymbol{\sigma}_0+\mathbf{D}_e \Delta \boldsymbol{\epsilon})$ or the deviatoric stresses $(s_{ij}^0+2G \Delta e_{ij})$, as shown in Fig. 6), which would occur if the response to $\Delta \boldsymbol{\epsilon}$ or Δe_{ij} were linear elastic. In view of the special features of Mises' yield surface in the deviatoric space, we can immediately define the direction of the vector of the incremental plastic strain, reach the yield surface through a radial path and determine the final deviatoric stresses \hat{s}_{ij} .

After examining all the *strain points*, a new vector $\Delta \boldsymbol{\lambda} \neq \mathbf{0}$ can be defined and another displacement vector \mathbf{U} can be computed (second iteration). Thus, different increments Δe_{ij} or Δe_{ij}^p will be considered at each *stress point* and different values of Δe_{ij}^p will be found.

The iterative process shall continue until a convenient norm is below a given tolerance η (*e.g.*, until $|\mathbf{U}_{i+1}-\mathbf{U}_i|/|\mathbf{U}_i|<\eta$, if \mathbf{U}_i and \mathbf{U}_{i+1} denote the displacement vectors computed at two consecutive iterations and $|\mathbf{v}|$ represents the Euclidean norm of a given vector \mathbf{v}).

Similar remarks can be made when linear isotropic or kinematic hardening is considered. In this case, it is necessary to take into account the radius increment or the displacement of the center of the spherical surface (*cf.* Fig. 7, where these quantities are shown by arrows that represent vectors whose components are Δs_{ij} , while the solid curves correspond to updated yield surfaces).

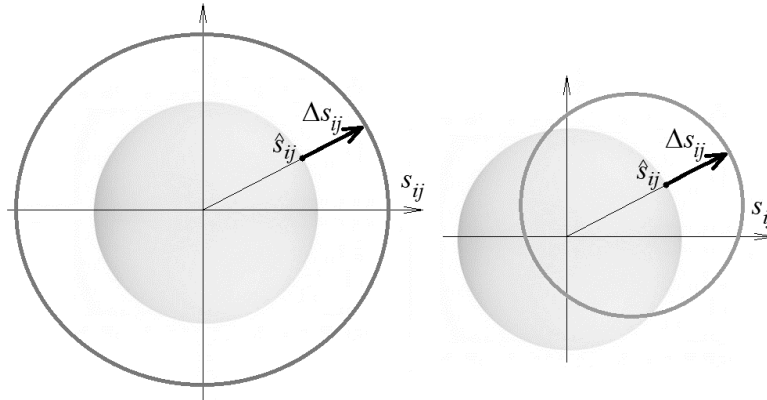


Figure 7. Mises' yield condition: isotropic and kinematic hardening.

As for the *backward-difference* scheme, the procedure is essentially the same, without significant changes with respect to the case of elastic-perfectly plastic materials. As obvious, a *hardening parameter* is needed, which plays the role of the stiffness g in the mechanical model of Fig. 4 and the consequent load-displacement plot of Fig. 5. This *hardening parameter*, which must be constant in the presence of linear hardening and will be denoted as $2G'$, shall establish a relationship between the increments Δs_{ij} and Δe_{ij}^p (as well as the parameter g introduced above is the ratio between the increment of the yield stress and the corresponding increment of the plastic strain in the case of uniaxial stress states).

Thus, at the end of each iteration, the final deviatoric stresses \hat{s}_{ij} acting on the slip devices and computed at each *strain point* is $(s_{ij}^0 + 2G(\Delta e_{ij} - \Delta e_{ij}^p) - 2G' \Delta e_{ij}^p)$ instead of $(s_{ij}^0 + 2G \Delta e_{ij} - 2G \Delta e_{ij}^p)$, as it happens in the case of elastic-perfectly plastic materials.

Finally, before concluding this Section, it might be useful to point out that the matrix \mathbf{L} introduced above must be substituted with a different matrix, say \mathbf{L}^* , when deviatoric stresses are considered. Indeed, \mathbf{L}^* shall be obtained from convenient submatrices \mathbf{L}_i^* , which can be defined by considering the equation

$$\sum_i \int \{\delta \mathbf{u}_i\}^T [-\mathbf{B}_i + \mathbf{B}_i^*]^T \mathbf{D}_i^* \boldsymbol{\Psi}_i \boldsymbol{\lambda}_i dV = \sum_i \{\delta \mathbf{u}_i\}^T \mathbf{L}_i^* \boldsymbol{\lambda}_i \quad (12)$$

instead of eqn. (10). Here, \mathbf{D}_i^* is a diagonal matrix whose non-zero entries are $2G$ and $[\mathbf{B}_i - \mathbf{B}_i^*]$ is a matrix that gives deviatoric strains when it is multiplied by the displacement vector \mathbf{u}_i .

Similarly, when the vector $\boldsymbol{\chi}_i$ is considered, we shall set $\boldsymbol{\chi}_i = \{ [-\mathbf{L}_i^*]^T \mathbf{u}_i - \mathbf{S}_i^* \boldsymbol{\lambda}_i - \mathbf{G}_i^* \boldsymbol{\lambda}_i \}$, where \mathbf{S}_i^* and \mathbf{G}_i^* are again diagonal matrices.

4. Some remarks about the *generalized forces*

If we consider structural systems characterized by uniaxial stress states, the vector $\{ -\mathbf{L}^T \mathbf{U} \}$ that gives axial forces acting on the structural elements does not create any particular problem when the yield condition is to be satisfied. In fact, the required information can be obtained immediately from the traditional stress-strain plots, since stresses simply correspond to axial forces divided by cross sectional areas and strains to elongations divided by initial lengths of the bars.

Instead, when multiaxial stress states occur, the correlation between yield functions (defined in the space of stresses or deviatoric stresses) and elastic domains in the space of the *generalized forces*

is not so obvious. Thus, it is necessary to investigate what happens in the case of finite elements, which are used for discrete models of structural systems characterized by multiaxial stress states. In this Section we will deal with this issue, by focusing on quadrangular finite elements (more specifically, eight-node rectangular elements). However, the extension to different elements (and, in general, to three-dimensional elements) is quite straightforward.

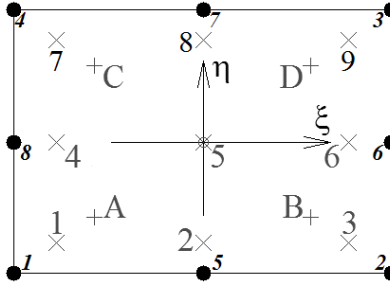


Figure 8. Rectangular finite element and possible Gauss points.

As already pointed out, it is typical to select *strain points* (i.e., points where we must satisfy the constitutive law), which usually coincide with *Gauss points* in the case of rectangular elements. For instance, we can make use of four points (A, B, C, D, whose non-dimensional coordinates ξ and η are $\pm 1/\sqrt{3}$) or nine points (1-9, whose non-dimensional coordinates are 0 and/or $\pm\sqrt{15}/5$). In principle, we might also consider the case of a single *strain point* (the center of gravity, that is point 5 in Fig. 8), but this choice would be quite unusual for eight-node quadrangular elements.

It is well known that, according to Gauss' method, an integral can be computed numerically, if we multiply the value of the integrand function at the selected points by convenient weights (one for each non-dimensional coordinate) and sum all the contributions. In view of some interesting features of the *generalized forces* discussed in this Section, we should take note of the fact that the weights are 2 when a single point is chosen, 1 when four points are chosen and 5/9 or 8/9 when nine points are chosen (8/9 for $\xi=0$ or $\eta=0$, 5/9 in the other cases).

Indeed, the *generalized forces* depend on the stress distribution and on zones of influence, which (in turn) depend on the weights assigned to each coordinate in the framework of Gauss' integration method. Therefore, when we need to introduce a *dissipation function* and/or establish a relationship between *generalized forces* and feasible stress states (defined on the basis of a *yield surface* in the space of stresses or deviatoric stresses), we must divide the *generalized forces* by an appropriate volume, say \tilde{V} , which can be obtained by means of the following simple formula in the case of the rectangular element in Fig. 8:

$$\tilde{V} = V w_{\xi} w_{\eta} / W \tag{13}$$

Here, V denotes the volume of the finite element, w_{ξ} and w_{η} are the weights assigned to ξ and η at the point where the given *generalized forces* have been computed, W represents the sum of the products ($w_{\xi} w_{\eta}$) at all the stress points.

Therefore, in the case of the single *strain point*, we have the obvious result $\tilde{V}=V$, since W coincides with the product ($w_{\xi} w_{\eta}$).

If four points are considered, the result is $\tilde{V}=V/4$, which is again absolutely obvious, since there is no reason why the zones of influence should be different in view of the evident symmetries. In fact, the product $(w_\xi w_\eta)$ is always equal to 1, while W (sum of all products) is equal to 4.

Instead, if we select nine points, \tilde{V} depends on the point where the *generalized forces* have been computed, since the product $(w_\xi w_\eta)$ can be equal to 64/81 or 25/81 or 40/81, while W is clearly equal to 324/81. In fact, we have $\xi=\eta=0$ at one point, $\xi=\pm\eta=\pm(\sqrt{15})/5$ at four points, $\xi=\pm(\sqrt{15})/5$ and $\eta=0$ or $\xi=0$ and $\eta=\pm(\sqrt{15})/5$ at four points.

It can be checked that these results are quite reasonable by studying a single element subjected to a uniform strain distribution, assuming a *plane-stress* state. For instance, we can focus on a rectangular eight-node finite element with length=400 mm, height=280 mm and thickness=1 mm. Hence, its volume is 112,000 mm³.

Now, assuming $E=200,000 \text{ Nmm}^{-2}$ and $\nu=0.3$, we can impose positive horizontal displacements of the right edge equal to 0.04 mm (*cf.* Fig. 8), positive horizontal displacements of the mid-points of the horizontal edges equal to 0.02 mm, upward vertical displacements of the lower edge equal to 0.0042 mm and downward vertical displacements of the upper edge also equal to 0.0042 mm. If all the other displacements are zero, we eventually end up with the strain components $\varepsilon_{11}=0.04/400=0.0001$ in the ξ -direction and $\varepsilon_{22}=-0.0084/280=-0.00003=-\nu \varepsilon_{11}$ in the η -direction. These values imply only one significant stress component, namely $\sigma_{11}=E \varepsilon_{11}=20 \text{ Nmm}^{-2}$. In addition we have the deviatoric stresses $s_{11}= 13.333 \text{ Nmm}^{-2}$ and $s_{22}=s_{33}= -6.666 \text{ Nmm}^{-2}$.

Now, we can take a look at Tab. 1 that shows the entries of the vectors $\mathbf{q}_i=-\mathbf{L}_i^T \mathbf{u}_i$ and $\mathbf{q}_i^*=-\mathbf{L}_i^{*T} \mathbf{u}_i$.

Number of strain points	Entries of the vector \mathbf{q}_i [N mm]	Entries of the vector \mathbf{q}_i divided by \tilde{V} [N mm ⁻²]	Entries of the vector \mathbf{q}_i^* [N mm]	Entries of the vector \mathbf{q}_i^* divided by \tilde{V} [N mm ⁻²]	\tilde{V} [mm ³]
1	2,240,000 0 0	20 0 0	1,493,333 -746,667 -746,667 0	13.3333 -6.6667 -6.6667 0	112,000
4	560,000 0 0	20 0 0	373,333 -186,667 -186,667 0	13.3333 -6.6667 -6.6667 0	28,000 (for the zone around any strain point)
9	442,469 0 0 172,839.5 0 0 276,543.2 0 0	20 0 0 20 0 0 20 0 0	294,979.4 -147,489.7 -147,489.7 0 115,226.3 -57,613.17 -57,613.17 0 184,362.1 -92,181.07 -92,181.07 0	13.3333 -6.6667 -6.6667 0 13.3333 -6.6667 -6.6667 0 13.3333 -6.6667 -6.6667 0	22,123.457 (for the zone around the center of gravity or strain point 5) 8,641.975 (for the zones around the strain points 1, 3, 7, 9) 13,827.16 (for the zones around the strain points 2, 4, 6, 8)

Table 1. Stresses and relevant *generalized forces* for a rectangular finite element.

Note that Tab. 1 shows three stress components ($\sigma_{11}, \sigma_{22}, \sigma_{12}$) and four deviatoric stress components ($s_{11}, s_{22}, s_{33}, s_{12}$), since they represent the significant terms of the relevant tensors in the presence of *plane stress* conditions. As for the values in the second and fourth column, they appear to be in full agreement with the above comments about the influence of the weights concerned with *Gauss' integration method*. In fact, each *generalized force* corresponds to the given uniaxial stress (20 Nmm⁻²) or a given deviatoric stress (13.333 Nmm⁻² or -6.666 Nmm⁻²) multiplied by a convenient volume \tilde{V} , which depends on the particular *strain point*.

As already pointed out, \tilde{V} (reported in the sixth column) coincides with the volume $V=112,000$ mm³ when we have a single *strain point* and is always equal to $V/4$ in the case of four *strain points*, because of obvious symmetries. Instead, there are some differences if we consider nine *strain points*, since Gauss' weights depend on the value of each non-dimensional coordinate.

Now, taking into account what happens in the presence of uniform stress distributions, we can immediately derive the rule to be applied when the constitutive law is to be enforced at a *strain point* and we need to reason in terms of *generalized forces*, instead of stresses or deviatoric stresses. The yield surface and/or the *dissipation function* to be considered are exactly the ones that we would define in terms of stresses or deviatoric stresses, provided that we multiply these stresses by the volume \tilde{V} concerned with the zone around the given *strain point*. This rule appears to be correct, since it gives exact results, when the numerical method is able to describe the real system without modelling errors (as happens, for instance, in the case of the uniform uniaxial stress discussed above).

For instance, if the initial yield surfaces in Fig. 7 are based on a yield stress equal to 300 Nmm⁻² (concerned with uniaxial stress states), their radii are $r=244.949$ Nmm⁻², as suggested by eqn. (11), in which $w_L=1/4(s_{11}^2+s_{22}^2+s_{33}^2)/G$, since w_L must be expressed as a function of the deviatoric stresses that correspond to the yield stress (say σ_{11}). So, when σ_{11} is equal to 300 Nmm⁻², we obtain $s_{11}=200$ Nmm⁻² and $s_{22}=s_{33}=-100$ Nmm⁻² (while $s_{ij}=0$ for $i \neq j$), which actually lead to a radius $r=244.949$ Nmm⁻².

In consequence, when we need to define the same surfaces in the space of the *generalized forces* and introduce the *tool* needed to enforce the constitutive law and/or define a convenient *dissipation function* by making use of these forces, we shall simply consider spherical elastic domains whose radii are $r\tilde{V}$ Nmm.

Alternatively and, definitely, in a more straightforward way, it is possible to derive the same results by considering some basic aspects concerned with the so-called *isoparametric elements* (e.g., generic quadrangles or quadrangles characterized by curved edges).

In this case, the same shape functions that depend upon the non-dimensional coordinates $\xi-\eta$ and provide the displacement of any element point when the nodal displacements are known, can be used to define the classical $x-y$ coordinates of any element point when the $x-y$ coordinates of the nodes are given.

Indeed, for a plane element we can set

$$x(\xi, \eta) = \sum_i \varphi_i(\xi, \eta) x_i \quad , \quad y(\xi, \eta) = \sum_i \varphi_i(\xi, \eta) y_i \quad (14a,b)$$

where, x_i and y_i denote the coordinates of the i -th node, while $\varphi_i(\xi, \eta)$ is the shape function that is equal to one at the i -th node and equal to zero at all the other nodes.

At this stage, it should be noted that the area $dA=dx dy$ of a surface element can be expressed in terms of infinitesimal increments of the non-dimensional coordinates by setting $dA=|\det[\mathbf{J}]|d\xi d\eta$, where $|\det[\mathbf{J}]|$ is the absolute value of the determinant of the *Jacobian matrix*, which is equal to $(\partial x/\partial \xi \partial y/\partial \eta - \partial x/\partial \eta \partial y/\partial \xi)$ for a plane system.

Clearly, for a rectangle whose horizontal and vertical sides are $2a$ and $2b$, respectively, we obtain $\det[\mathbf{J}]=ab$, since $\xi=x/a$ and $\eta=y/b$. Therefore, instead of using eqn. (13), it is possible to set

$$\tilde{V} = |\det[\mathbf{J}]| h w_{\xi} w_{\eta} \tag{15}$$

if the parameter h denotes the element thickness. In fact, the product $(|\det[\mathbf{J}]|h)$ is equal to abh or $V/4$. In consequence, we immediately see that $\tilde{V}=V$ with a single *strain point* (since $w_{\xi}=w_{\eta}=2$), while $\tilde{V}=V/4$ with four *strain points* (since $w_{\xi}=w_{\eta}=1$).

Instead, when nine *strain points* are considered, we should observe that W in eqn. (13) is equal to $324/81$ (i.e., is equal to 4), since we have $w_{\xi}w_{\eta}=c/81$, with $c=64$ or 25 or 40 . Thus, eqn. (15) leads to the same result given by eqn. (13) in view of the relationship $|\det[\mathbf{J}]|h=V/4=V/W$.

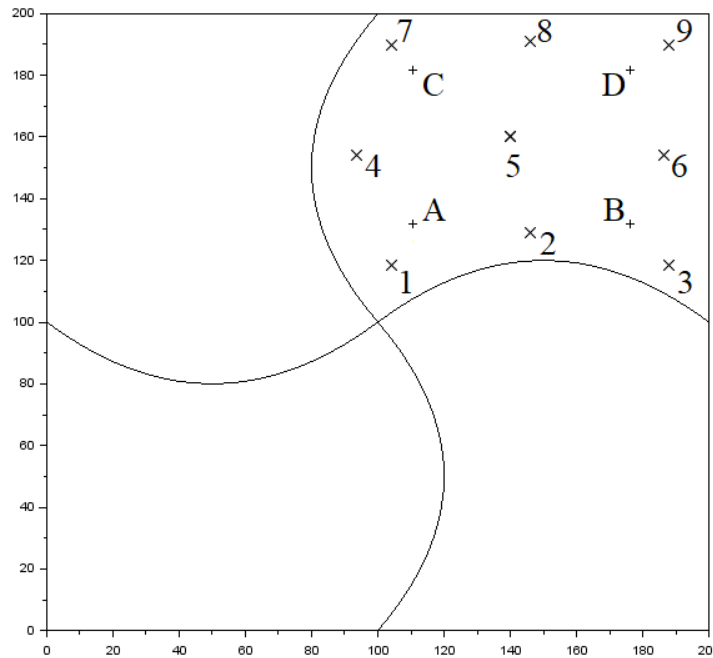


Figure 9. Mesh of a plane system based on eight-node elements (total area:200x200mm²).

At this stage, it should be noted that the approach based on the use of the Jacobian matrix becomes absolutely necessary when isoparametric *distorted elements* (as shown, e.g., in Fig. 9) are considered and the *influence regions* around the *strain points* cannot be determined in a straightforward way by drawing obvious conclusions suggested by the simple geometric configurations that characterize rectangular elements.

For instance, it is possible to prove that eqn. (15) provides correct values of the volumes \tilde{V} for the eight-node elements in Fig. 9 by considering a uniform strain distribution for the plane system shown in the picture. To this aim we imposed zero horizontal displacements to the nodes along the left edge and horizontal displacements equal to 0.1 mm to the nodes along the right edge. In addition, a zero vertical displacement was imposed to the mid-point of the left edge in order to

prevent rigid-body motion. Therefore, by setting $E=200,000 \text{ Nmm}^{-2}$ and $\nu=0.3$, we obtained a uniform distribution of normal horizontal stresses $\sigma_{11}=E\varepsilon_{11}=E \cdot 0.1/200=100 \text{ Nmm}^{-2}$ assuming a linear-elastic response and a *plane-stress* state. Instead, in the case of *plane-strain* conditions, the equations $\sigma_{22}=0$ (as required by the boundary conditions) and $\varepsilon_{33}=(\sigma_{33}-\nu\sigma_{11})/E=0$ imply that $\sigma_{11}=E\varepsilon_{11}+\nu\sigma_{33}=E\varepsilon_{11}/(1-\nu^2)=109.89 \text{ Nmm}^{-2}$ and $\sigma_{33}=32.967 \text{ Nmm}^{-2}$.

Hence, we eventually have the deviatoric stresses $s_{11}=66.667 \text{ Nmm}^{-2}$ and $s_{22}=s_{33}=33.333 \text{ Nmm}^{-2}$ for the *plane-stress* state and $s_{11}=62.271 \text{ Nmm}^{-2}$, $s_{22}=-\sigma_h=-47.619 \text{ Nmm}^{-2}$ and $s_{33}=-14.652 \text{ Nmm}^{-2}$ for the *plane-strain* state (if σ_h denotes the hydrostatic stress).

These values of the deviatoric stresses can be obtained at any *strain-point* of any element if we consider, for each element, the vector $\mathbf{q}_i^*=-\mathbf{L}_i^{*T} \mathbf{u}_i$ and divide each entry by the appropriate volume \tilde{V} determined through eqn. (15), as shown in Tab. 2.

Strain point	s_{11}	q_1^*	s_{11}	q_1^*	s_{33}	q_3^*	\tilde{V} [mm ³]
	[N mm ⁻²] (<i>pl. stress</i>)	[N mm] (<i>pl. stress</i>)	[N mm ⁻²] (<i>pl. strain</i>)	[N mm] (<i>pl. strain</i>)	[N mm ⁻²] (<i>pl. strain</i>)	[N mm] (<i>pl. strain</i>)	
A	66.667	185819.56	62.271	173567.72	-14.652	-40839.464	2787.293
B	66.667	157777.78	62.271	147374.85	-14.652	-34676.435	2366.667
C	66.667	157777.78	62.271	147374.85	-14.652	-34676.435	2366.667
D	66.667	165291.55	62.271	154393.21	-14.652	-36327.813	2479.373
1	66.667	66662.683	62.271	62267.341	-14.652	-14651.139	999.9402
2	66.667	71111.111	62.271	66422.466	-14.652	-15628.816	1066.667
3	66.667	49135.802	62.271	45896.079	-14.652	-10799.077	737.0370
4	66.667	90864.198	62.271	84873.152	-14.652	-19970.153	1362.963
5	66.667	126419.75	62.271	118084.38	-14.652	-27784.561	1896.296
6	66.667	90864.198	62.271	84873.152	-14.652	-19970.153	1362.963
7	66.667	49135.802	62.271	45896.079	-14.652	-10799.077	737.0370
8	66.667	71111.111	62.271	66422.466	-14.652	-15628.816	1066.667
9	66.667	51362.008	62.271	47975.502	-14.652	-11288.353	770.4301

Table 2. Deviatoric stresses and relevant *generalized forces* for the top-right element in Fig. 9.

For the sake of brevity, in Tab. 2 we only report a few results concerned with the top-right element in Fig. 9 when four or nine *strain-points* are considered. Namely, for the *plane-stress* case we simply give the first entry of \mathbf{q}_i^* (say q_1^*) since the values of the other terms is obvious. Instead, for the *plane-strain* case the table gives the values of the first and third entry (q_1^* and q_3^* , which are obviously assumed to correspond to s_{11} and s_{33}). By examining the values of \tilde{V} concerned with each *strain-point* and listed in the last column, it can be easily checked that each deviatoric stress actually corresponds to the pertinent value of q_1^* or q_3^* divided by the relevant volume \tilde{V} .

Finally, it is worth noting that eqn. (15) cannot be applied to this kind of elements, if we make use of a single *strain-point* (a choice, which, anyway, would be quite unusual for eight-node elements, as pointed out above). As a matter of fact, when we compute the derivatives of x and y with respect to ξ and η for $\xi=\eta=0$, their values only depend on the coordinates of the element mid-points. More specifically, if we assume that the element nodes are numbered as shown in Fig. 8, we obtain

$\partial x/\partial \zeta=(x_6-x_8)/2$, $\partial y/\partial \eta=(y_7-y_5)/2$, $\partial x/\partial \eta=(x_7-x_5)/2$, $\partial y/\partial \zeta=(y_6-y_8)/2$ when for $\zeta=\eta=0$. Therefore, we eventually find $|\det[\mathbf{J}]|=[(x_6-x_8)(y_7-y_5)-(x_7-x_5)(y_6-y_8)]/4$.

This result is not surprising in the case of eight-node elements, because the x - y coordinates of any point are given by eqns. (14), if x_i and y_i denote the coordinates of its nodes (and the shape functions φ_i are properly defined). For instance, if the i -th node corresponds to the left bottom node of any element in Fig. 9 (and its coordinates are $\zeta=\eta=-1$), we must set $\varphi_i(\zeta, \eta)=-\frac{(\zeta-1)(\eta-1)(\zeta+\eta+1)}{4}$. Therefore, when we compute the derivatives, we obtain $\partial \varphi_i/\partial \zeta=-\frac{(\eta-1)(\zeta+\eta+1)}{4}-\frac{(\zeta-1)(\eta-1)}{4}$ and $\partial \varphi_i/\partial \eta=-\frac{(\zeta-1)(\zeta+\eta+1)}{4}-\frac{(\zeta-1)(\eta-1)}{4}$, which are obviously equal to zero for $\zeta=\eta=0$ (and the same result can be obtained for the shape functions that must be multiplied by the coordinates of the other corner points).

Instead, if the i -th node corresponds to mid-point of the lower edge of any element in Fig. 9 (whose coordinates are $\zeta=0$ and $\eta=-1$), we have $\varphi_i(\zeta, \eta)=\frac{(\zeta^2-1)(\eta-1)}{2}$. In consequence, the relevant derivatives become $\partial \varphi_i/\partial \zeta=\zeta(\eta-1)$ and $\partial \varphi_i/\partial \eta=\frac{(\zeta^2-1)}{2}$, which are equal to 0 and -0.5 for $\zeta=\eta=0$ (and similar results are obtained, if we consider the shape functions that must be multiplied by the coordinates of the other mid-points: one derivative is zero, while the other one is equal to ± 0.5).

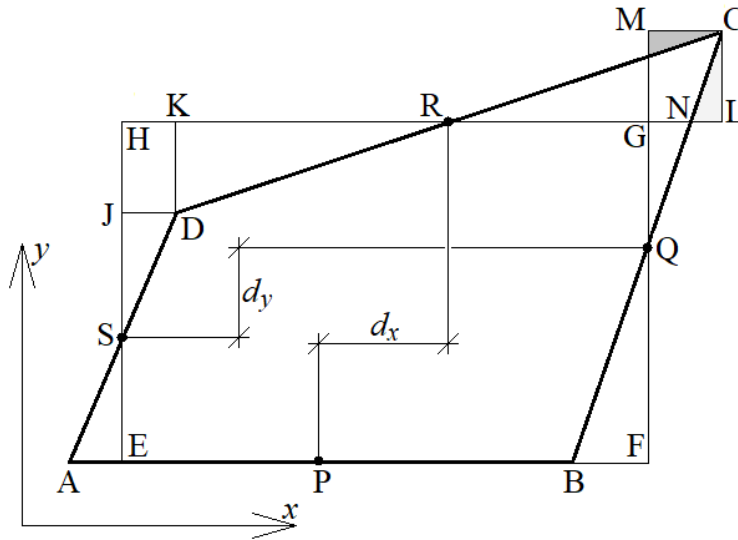


Figure 10. Correlation between a quadrilateral and the Jacobian matrix computed for $\zeta=\eta=0$.

Thus, the absolute value of the Jacobian matrix gives the element area divided by 4 and allows one to find the correct volume only in the case of quadrilaterals (cf. Fig. 10). Instead, when points such as P, Q, R, S in this figure correspond to the mid-points of elements characterized by curved edges, the result given by eqn. (15) would obviously be wrong and \tilde{V} should be determined by computing the integral $(\int dA)$ through Gauss' method.

For the sake of simplicity the side AB of the quadrilateral in Fig. 10 is parallel to the x -axis. Hence, it is quite easy to check that its area is equal to the absolute value of the Jacobian matrix multiplied by 4 when $\zeta=\eta=0$. In fact, the product $[(x_6-x_8)(y_7-y_5)]$ gives the area of the rectangle EFGH and we can notice the following interesting properties:

- the polygon EBQGRDS is in common between the rectangle EFGH and the quadrilateral ABCD

- the area of the triangle AES (which only belongs to the quadrilateral) is equal to the area of the triangle SDJ (which only belongs to the rectangle EFGH)
- the areas of the triangles DRK and BFQ (which only belong to the rectangle EFGH) are equal to the areas of the triangles RLC and QCM (which only belong to the rectangle EFGH, with the exception of the areas of the light-grey and dark-grey triangles, respectively)
- since the area of the quadrangle GNCM has been considered twice, eventually the area of the quadrilateral ABCD turns out to be equal to the area of the rectangle EFGH minus the areas of the rectangles JDKH and GLCM
- the segments DK and LC are equal to d_y , which (in turn) is equal to $(y_6 - y_8)$, while the sum of the segments HK and GL is equal to d_x , which (in turn) is equal to $(x_7 - x_5)$

5. Closing remarks

This paper has revisited a non-traditional *internal variable* formulation of the incremental elastic plastic problem and put some emphasis on the convergence properties of a numerical approach based on the *backward-difference* concept. Within this context, it has been pointed out that a key role is played by a convenient set of *generalized forces*, which give a contribution to an objective function, whose minimum point corresponds to the solution of the structural problem (if the material is stable in *Drucker's sense*), so that convergence is guaranteed for iterative procedures that steadily reduce the value of that function. It has also been noted that, so far, the basic features of those *generalized forces* have been completely ignored, even though there exist some non-trivial aspects related to their intrinsic links with *yield functions* and/or *dissipation functions*, which are obviously required to satisfy the constitutive law. Indeed, these functions (usually expressed in terms of stresses or deviatoric stresses) are to be defined in terms of *generalized forces*.

More specifically, the relationship between *generalized forces* and *yield functions* or *dissipation functions* is quite straightforward in the case of uniaxial stress states and finite elements characterized by a uniform stress distribution, which have been implicitly considered until now in the existing literature related to the *internal variable* approach discussed here. Instead, the correct definition of *yield functions* and *dissipation functions* is far from being a trivial problem in the more general cases, especially in the presence of isoparametric elements, and this issue has been thoroughly investigated in the paper, for the first time to the best of the authors' knowledge.

6. References

- [1] J.B. Martin, An Internal Variable Approach to the Formulation of Finite Element Problems in Plasticity, in *Physical Non-Linearities in Structural Analysis* (edited by J. Hult and J. Lemaitre). Springer-Verlag, Berlin, 1981.
- [2] J.B. Martin, A. Nappi, An internal variable formulation for perfectly plastic and linear hardening relations in plasticity, *European Journal of Mechanics, A/Solids*, 9, 107-131, 1990.
- [3] A. Nappi, Application of convex analysis concepts to the numerical solution of elastic plastic problems by using an internal variable approach, *Engineering Optimization*, 18, 79-92, 1991.
- [4] S. Rajgelj, C. Amadio, A. Nappi, An internal variable approach applied to the dynamic analysis of elastic-plastic structures, *Earthquake Engineering and Structural Dynamics*, 22, 885-903, 1993.